

Adsorption of Weak Polyelectrolytes to an Oppositely Charged Langmuir Film: Change in the Conformation of the Adsorbed Molecules and Saturation of the Ionization Degree

Laurianne Vagharchakian,[†] Bernard Desbat,[‡] and Sylvie Hénon^{*,†}

Laboratoire de Biorhéologie et Hydrodynamique Physicochimique, CNRS UMR7057, Matière et Systèmes Complexes, FR2438 Université Paris 7, case courrier 7056, 2 place Jussieu, 75251 Paris Cedex 05, France, and Laboratoire de Physico-Chimie Moléculaire, CNRS UMR 5803, Université Bordeaux 1, 33405 Talence Cedex, France

Received July 16, 2004; Revised Manuscript Received August 30, 2004

ABSTRACT: We have studied the adsorption of a weak flexible polyelectrolyte, poly(acrylic acid), at an oppositely charged surface, the surface of water covered with a Langmuir film of dimethyldioctadecylammonium bromide. The surface charge density and the polymer ionization degree α were conveniently varied by varying respectively the density σ of the Langmuir film and the pH of the polyelectrolyte solution. By infrared spectroscopy we evidenced a change in the mean orientation of the adsorbed chains when increasing the surface charge density, from parallel to the surface for $\sigma < \sigma_0$ to perpendicular to the surface for $\sigma > \sigma_0$. A signature of this regime change also appears in the compression elastic modulus. The value of σ_0 scales as α at low α , as predicted by theory, but saturates when increasing α , presumably because of a saturation of the polyelectrolyte charge fraction.

Introduction

The adsorption of charged polymers (polyelectrolytes) onto oppositely charged surfaces plays a central role in a wide range of biological and industrial processes, such as cell adhesion, wastewater treatment, the stabilization of paints and of food emulsions, etc. It has been the subject of a tremendous amount of experimental and theoretical work within the past 40 years,^{1–4} with an increasing number of experimental techniques (such as X-ray and neutron reflectivity,⁵ ellipsometry,⁶ second harmonic generation,⁷ IR spectroscopy,⁸ etc.) and of theoretical methods (field calculations, scaling arguments, numerical simulations).⁴ For most of the applications thick adsorbed layers are desirable, but very thin layers are in general observed.⁹ A recent theoretical work^{10,11} predicted a transition in the conformation of the adsorbed chains, from a 2-d layer at low surface charge density to a 3-d layer at high surface charge density.

We were able to evidence this transition in a system in which both the charge density of the surface and the linear charge density of the polyelectrolyte could be varied: weak polyelectrolytes adsorbing from a dilute aqueous solution onto its free surface, charged by the presence of a Langmuir film.

Experimental Section

Chemicals. The amphiphile molecule for the preparation of Langmuir films is dimethyldioctadecylammonium bromide (DODA). It was purchased from Sigma-Aldrich and used without further purification (purity ~99%). The polyelectrolyte is poly(acrylic acid) (PAA), bought from Sigma-Aldrich, either in an acidic form PAAH, average molecular weight ~5000 g (average degree of polymerization: ~69), or in a neutralized form PAA⁻Na, average molecular weight ~5100 g (average degree of polymerization: ~54). The polyelectrolyte solutions were made in ultrapure water from a Millipore–Simplicity

system (resistivity 18.2 M Ω cm). Their concentration was about the same in all the experiments: 1×10^{-4} – 2×10^{-4} mol of monomers per L (7.2–14.4 mg of poly(acrylic acid) per kg of water). The pH of the solutions was adjusted by addition of NaOH (Prolabo, Normapur) to the PAAH solutions or HCl (Prolabo, Normapur) to the PAA⁻Na solutions. As the pH is increased, the ionization degree α of the polymer (the fraction of dissociated COOH groups) increases. No additional salt was added to the solutions. PAAH is close to theta solvent conditions in water at room temperature.¹²

Langmuir Film Preparation and Isotherms Recording. The surface pressure measurements were held in a home-built thermostated Langmuir trough, 13×30 cm², coated with Teflon and equipped with a Wilhelmy plate system (R&K, Germany, resolution 0.1 mN/m). The experimental procedure was as follows: pure water or a PAA solution is poured in the trough, its free surface is cleaned by a suction device, the value of the surface pressure on the Wilhelmy plate system is then set to 0, and a controlled quantity of a solution of DODA in chloroform (concentration ~0.5 mg/mL) is deposited at the surface; after waiting a few minutes for the evaporation of chloroform, the surface pressure is recorded.

Compression Elasticity Measurements. The compression elastic modulus of a film is defined as $\epsilon = -S d\pi/dS = -A d\pi/dA = \sigma d\pi/d\sigma$; π is the surface pressure, S the total area of the film, A the area per amphiphile molecule, and $\sigma = 1/A$ the density of the film. The compression moduli were calculated directly from the isotherms. For the calculation, the isotherms were first “smoothed out” by averaging the measurements over a few $\text{\AA}^2/\text{molecule}$. From these smoothed data, ϵ was calculated as $\epsilon \approx -A[\pi(A + \Delta A/2) - \pi(A - \Delta A/2)]/\Delta A$, with $\Delta A \approx 5 \text{ \AA}^2/\text{molecule}$.

Brewster Angle Microscopy. The technique allows to directly visualize inhomogeneities on a microscopic scale in monomolecular films at the air–water interface. The instrument we used in this study was described elsewhere in detail.¹³ The size of the images is about $300 \times 400 \text{ }\mu\text{m}^2$, with a lateral resolution of about $1 \text{ }\mu\text{m}$. For the Brewster angle microscopy (BAM) experiments, we used a home-built Langmuir trough, 15.5×50 cm², coated with Teflon.

PM-IRRAS. The polarization modulated infrared reflection adsorption spectroscopy (PM-IRRAS) spectra have been recorded following the experimental procedure previously described.¹⁴ Each PM-IRRAS spectrum shown in this work is the normalized difference between the PM-IRRAS spectrum of the

[†] Université Paris 7.

[‡] Université Bordeaux 1.

* Corresponding author. E-mail: henon@ccr.jussieu.fr.

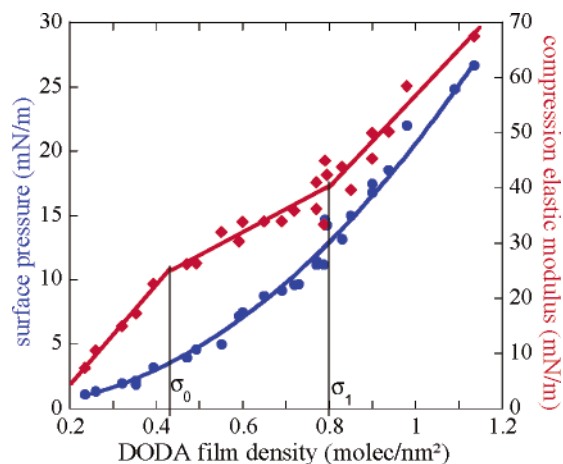


Figure 1. Surface pressure π (disks) and compression elastic modulus ϵ (diamonds) of Langmuir films of DODA at the surface of PAAH solutions, 1.7×10^{-4} mol of monomers/L, pH ≈ 4.8 , $T \approx 24$ °C, as a function of the DODA film density σ . The fit of π by a power law (σ^α , $\alpha \approx 2.08$), and the best linear fits of ϵ are also shown.

DODA film on the PAA solution and the PM-IRRAS spectrum of the corresponding PAA solution (without DODA film). The method is sensitive both to the presence of molecules at the water surface and to their orientation.¹⁴ The wavenumber of a band in an IR spectrum is characteristic of each chemical bond and of its surrounding. The intensity of a PM-IRRAS band is proportional to the quantity of molecules present at the surface and to a function of their orientation. The sign of the band depends on the angle γ between the absorption moment and the normal to the water surface. It is positive if $\gamma > 38^\circ$ (absorption moment close to the water surface) and negative if $\gamma < 38^\circ$ (absorption moment close to the water surface normal).

Results and Discussion

Low Ionization Degree. The results about the adsorption of PAA to a DODA film from a solution pH = 4.8 (ionization degree of PAA $\alpha \approx 0.12$) were described in a previous paper.¹⁵ We observed that the adsorption is slow (a few hours). The adsorption isotherm $\pi_{eq}(\sigma)$ was constructed point by point, by depositing a known density σ of DODA molecules at the surface of a PAA solution, and waiting for the surface pressure to reach its equilibrium value π_{eq} . The compression modulus ϵ was as well measured one point at a time, either by a fast compression from equilibrium or by the capillary waves technique.¹⁵ Figure 1 shows the measured values of π_{eq} and of ϵ as a function of the DODA film density σ . π_{eq} scales as σ^2 in the entire studied range (0.20–1.1 molecules/nm²). On the contrary, three regimes can be distinguished in the $\epsilon(\sigma)$ curve. The first regime change ($\sigma = \sigma_0 \approx 0.4$ molecule/nm²) was interpreted as a possible signature of a transition from a two-dimensional adsorbed layer for $\sigma < \sigma_0$ to three-dimensional adsorbed layer for $\sigma > \sigma_0$, as predicted by theory.^{10,11,15} The second regime change ($\sigma = \sigma_1 \approx 0.8$ molecule/nm²) corresponds to the transition from a regime in which the elasticity is dominated by the contribution of the adsorbed polymers to a regime in which both DODA molecules and adsorbed polymers contribute to ϵ .¹⁵

We now describe new results obtained by surface infrared spectroscopy. Figure 2a shows infrared absorption spectra of PAAH and PAANa solutions in water. (In these spectra the absorption of water has been removed by subtraction.) The absorption bands relative to the basic form are the carboxylate antisymmetric (ν_a

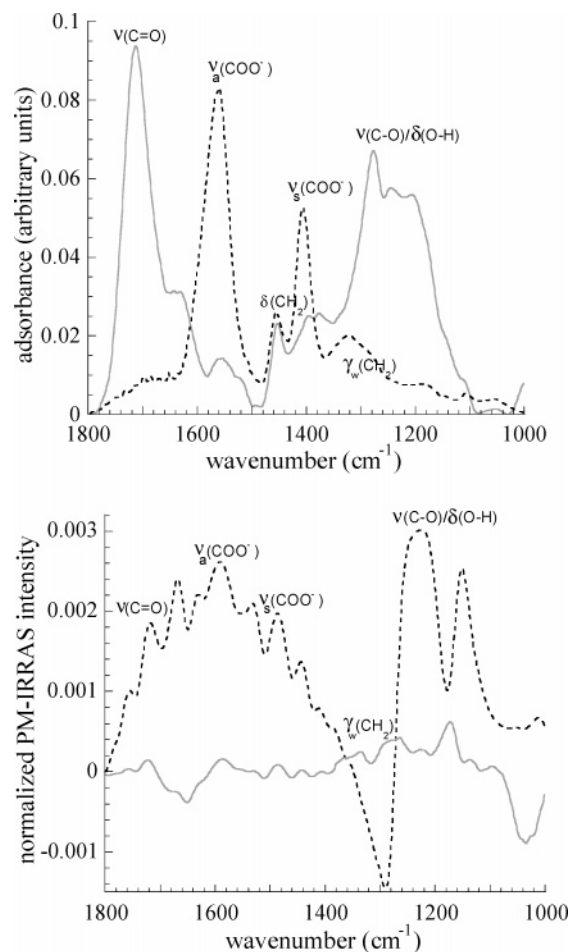


Figure 2. (a) Absorbance of PAAH (plain line) and PAANa (dashed line) in solution in water. (b) PM-IRRAS spectra of PAAH adsorbed at DODA Langmuir films from a PAAH solution, 1.7×10^{-4} mol of monomers/L, pH ≈ 4.8 , $T \approx 20$ °C. Plain line: DODA film density $\sigma = 0.35$ molecule/nm²; dashed line: $\sigma = 0.55$ molecule/nm².

COO⁻) and symmetric (ν_s COO⁻) stretching vibration bands, located at 1560 and 1405 cm⁻¹, respectively.¹⁶ The absorption bands relative to the acid form are the carbonyl stretching vibration mode (ν C=O) at 1720 cm⁻¹ and three bands between 1200 and 1280 cm⁻¹ corresponding to interacting C–O stretching (ν C–O) and O–H deformation (δ OH) modes.¹⁶ The band located at 1455 cm⁻¹ corresponds to the CH₂ bending vibration (δ CH₂).¹⁶ Finally, the band in the 1325 cm⁻¹ region corresponds mainly to CH₂ “wagging” (γ_w CH₂),¹⁶ a collective vibration of the CH₂ groups along the polymer chain.

Figure 2b shows PM-IRRAS spectra obtained from mixed DODA–PAA films for two different DODA film densities, 0.35 and 0.55 molecules/nm², both about 200 min after deposition of the DODA film. The only absorption band related to DODA in the 1000–1800 cm⁻¹ region is the CH₂ deformation band, at around 1470 cm⁻¹, but it is too weak to be observed in the presented spectra. The spectra show the absorption bands related to both the basic and the acid forms of PAA. The intensity of the C=O stretching band (with respect to the baseline) is weak as compared to the intensities of the bands related to the C–O–H group, while in the solution spectrum their intensities have the same order of magnitude (Figure 2a). Using the PM-

IRRAS selection rule,¹⁴ this shows that the angle between the C=O groups and the surface normal is probably close to 38° (a little higher, since the band is positive), while the C–O and O–H bonds are preferentially oriented in the surface plane. On the contrary, the carboxylate antisymmetric and symmetric stretching bands have relative intensities comparable to what is observed in bulk (Figure 2a). Since the corresponding transition moments are orthogonal to each other, the COO[−] groups either lie in the surface plane or have a random orientation. In principle, the ionization degree α of the adsorbed polymer may be deduced from the relative intensities of the bands related to the COOH and COO[−] groups.¹⁷ Unfortunately, it is not possible here because of the difference in the orientations of the two groups with respect to the surface.

There are two main differences between the two spectra of Figure 2b. First, in the spectrum at low density (0.35 molecule/nm²), all the bands are positively oriented with respect to the baseline. That shows that the angles between all the corresponding transition moments and the surface normal are higher than the “magical” angle 38° or have a random orientation. On the contrary, in the spectrum at higher density (0.55 molecule/nm²), two bands are negatively oriented: the CH₂ wagging band, located at 1295 cm^{−1}, and one of the C–O–H bands, located at 1190 cm^{−1}. This is perfectly consistent with a change in the orientation of the adsorbed polymers, from lying flat at the surface for $\sigma < \sigma_0$ (positive orientation of the CH₂ wagging band) to forming a 3D adsorbed layer for $\sigma > \sigma_0$, with a mean orientation of the chains orthogonal to the surface (negative orientation of the CH₂ wagging band). Second, the spectrum at low density shows a normal dip at 1650 cm^{−1}, which is due to the refractive index dispersion of water in this spectral domain,¹⁴ while the spectrum at high density shows a very large positive baseline in the 1800–1400 cm^{−1} region. This could as well be the signature of a difference in the organization of the adsorbed PAA layers. The dip at 1650 cm^{−1} in the PM-IRRAS spectra appears when the sample is formed of separate layers,¹⁴ as would be the case for adsorbed polymers lying flat at the surface. On the contrary, for a diffuse layer (as would be the case for an adsorbed 3D layer containing water) the PM-IRRAS signal is also sensitive to the change in the optical indices of water near its absorption bands at the interface. The change in the baseline in the 1600 cm^{−1} region could also correspond to a very wide band in this region due to the formation of strong H bonds, as is observed in the IR spectra of carboxylate salts.¹⁸

The flat orientation could be an out-of-equilibrium state of the adsorbed molecules. A change in the orientation of the adsorbed molecules was indeed observed during the adsorption of PAA to a DODA film with a density a little higher than σ_0 : $\sigma = 0.55$ molecule/nm². Figure 3 shows the corresponding PM-IRRAS spectra. In the first spectrum, taken 80 min after deposition of the DODA film on the PAA solution, all the bands are positively oriented with respect to the baseline. On the contrary, in the second spectrum, taken 210 min after the beginning of the experiment, two bands are negatively oriented: the orientation of the adsorbed polymers changes during the adsorption, from parallel to the surface to orthogonal to the surface. Nevertheless, the adsorption of PAA is slow: for $\sigma = 0.55$ molecule/nm² the adsorbed quantity reaches its

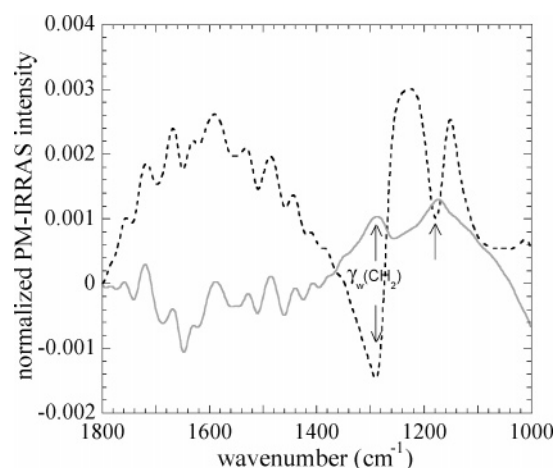


Figure 3. PM-IRRAS spectra of PAAH adsorbed at a DODA Langmuir film $\sigma = 0.55$ molecule/nm²: plain line, 80 min after the deposition of the DODA film at the surface of the PAAH solution; dashed line, 210 min after the deposition of the film. Two bands (indicated by arrows) have different signs in the two spectra.

equilibrium value within ~ 4 h.¹⁵ The amount of polymers adsorbed in 80 min is probably low enough to allow a flat orientation of the chains, while in 210 min, it has exceeded the value imposing a 3D layer. Furthermore, for $\sigma < \sigma_0$, the orientation of the adsorbed polymers remains flat for the entire observation time (which could not exceed about 200 min). Finally, the expected change in the orientation of the polymer during adsorption is the other way round: first a rapid adsorption of coils, followed by a slow reconfiguration to extended chains. Such a behavior has indeed been observed,^{7,19} but at time scales (a few seconds to a few minutes) beyond our experimental resolution.

Thus, the PM-IRRAS experiments confirm that the regime change in the elastic modulus at $\sigma = \sigma_0$ corresponds to a change in the orientation of the adsorbed polymers.

Intermediate Ionization Degree. We looked for the same regime change for other values of the ionization degree, using the same techniques: measurements of surface pressure and compression modulus and PM-IRRAS.

Isotherms as a Function of Temperature. For pH > 5 , the adsorption of the polyelectrolytes is more rapid than at low pH: it only takes a few minutes. Isotherms $\pi(\sigma)$ could be obtained at one time by a (relatively) slow compression of the film. The compression rate was about 15 mm² s^{−1} or about 5 Å² molecule^{−1} min^{−1}.

Figure 4a,b shows isotherms of DODA on pure water and on solutions of PAAH pH = 7 at several different temperatures between ~ 11 and 23 °C. The pH was adjusted either by adding NaOH to a PAAH solution or by adding HCl to a PAAHNa solution. The isotherms of DODA on pure water are similar to the ones found in the literature.^{5,20,21} At low density, the surface pressure is very low, and the film shows a gas–liquid expanded (LE) coexistence, as confirmed by Brewster angle microscopy. For $\sigma \approx 0.8$ molecule/nm², the film enters the pure LE phase, and the surface pressure begins to increase. A kink in the isotherms, for $\sigma \approx 1.33$ molecule/nm² and $\pi \approx 20$ mN/m at 23 °C, is the signature of a first-order phase transition between the LE and the LC (liquid condensed) phases. A first-order transition is expected to appear as a plateau in the isotherm. Here there are only kinks in the isotherms for several

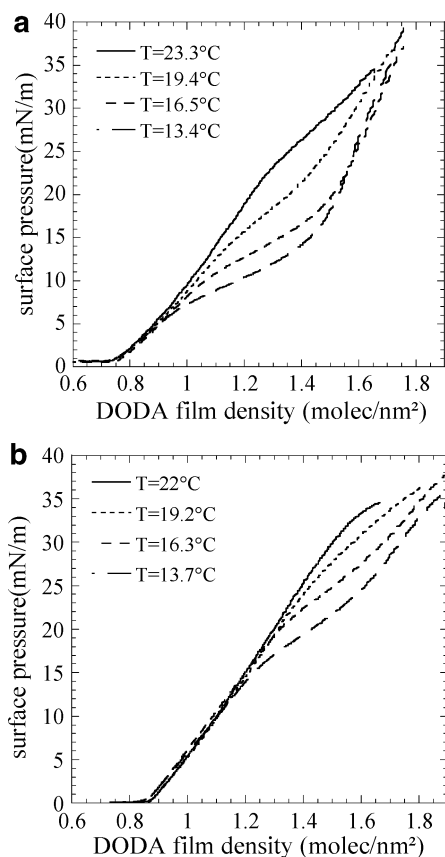


Figure 4. Isotherms of DODA at different temperatures: (a) on pure water; (b) on PAAH solutions, 10^{-4} mol of monomers/L, pH \approx 7.

reasons. First, the DODA we used is only 99% pure: the film is a mixture, and the transition plateau is deformed by the presence of impurities. Second, the long-range electrostatic repulsions between the molecules prevent the plateau from being completely flat. Finally, the counterion of the ammonium head, OH^- , seems to penetrate the alkyl part of the DODA molecule, thus increasing repulsions between the molecules;^{20,21} when using another counterion, for instance Cl^- , in concentration as low as 0.1 mM, we have checked that the plateau is much more flat and at a lower surface pressure. On the isotherms shown in Figure 4a, the transition “plateau” is all the more pronounced, wide, and at low pressure, as the temperature is low. On the contrary, the isotherm is almost independent of the temperature before the LE/LC transition. These are classical results for the LE phase and the LE/LC transition in a Langmuir film. The LE/LC phase coexistence can be observed with Brewster angle microscopy: Figure 5a shows LC domains growing in the LE phase, in that region of the isotherm. The LC domains are fractal or perhaps dendritic. This particular shape probably comes from the combination of two effects: first, the presence of impurities in DODA gives an impurities-diffusion-limited growth of the domains (which leads to fractals or dendrites), and second, the high viscosity of the LC phase prevents the domains from relaxing rapidly toward their equilibrium round shape.

Figure 4b shows isotherms of DODA on PAAH solutions (0.1 mM) at different temperatures. The isotherms have the same general feature as the ones on pure water: at low DODA film density a gas–LE coexistence is observed, then a pure LE phase, a LE–LC transition,

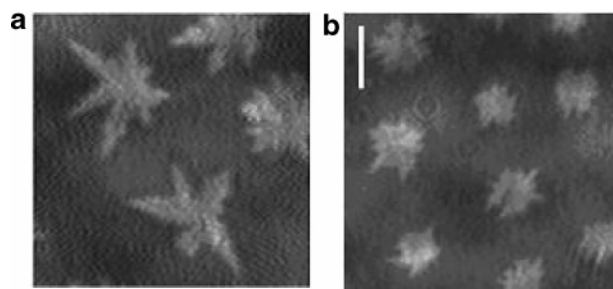


Figure 5. Brewster angle microscope images of DODA films at $\sigma = 1.6$ molecules/ nm^2 , $T \approx 20^\circ\text{C}$ (a) at the surface of pure water and (b) at the surface of a PAAH solution, 10^{-4} mol of monomers/L, pH \approx 7. The bar represents 25 μm .

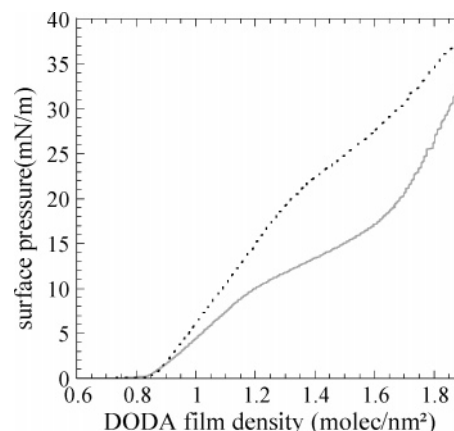


Figure 6. Isotherms of DODA on pure water (plain line) and on a PAAH solutions, 10^{-4} mol of monomers/L, pH \approx 7 (dashed line), at $T \approx 16.5^\circ\text{C}$.

and finally a pure LC phase. At high temperatures, the LE–LC transition does not clearly appear on the isotherms. However, it can be observed with Brewster angle microscopy, as shown in Figure 5b. As for DODA films on pure water, the isotherms depend on the temperature only in the LE/LC transition region.

For a more precise comparison, Figure 6 shows together isotherms of DODA on pure water and on a solution of PAA pH = 7 at the same temperature, $\sim 16.5^\circ\text{C}$. The isotherm on the polyelectrolyte solution differs from the one on pure water. That shows that some polyelectrolyte has adsorbed at the surface, replacing the counterions of DODA. There are two main differences between the isotherms: (i) the slope of the isotherm in the LE region is higher with the polyelectrolyte than on water (the LE phase is less compressible, as will be discussed later); (ii) the LE–LC transition is shifted toward higher density and higher surface pressure ($\Delta\sigma_{\text{LE-LC}} \approx 0.2$ molecule/ nm^2 , $\Delta\pi_{\text{LE-LC}} \approx 10\text{--}12$ mN/m). The isotherms converge in the LC phase. Both $\Delta\sigma_{\text{LE-LC}}$ and $\Delta\pi_{\text{LE-LC}}$ are almost independent of T .

In conclusion, the isotherms of DODA on PAA solutions, at pH > 5 , look like the ones on pure water: they show the same phase transitions. This restricts the range of σ values which can be explored. For instance, on the gas–LE plateau ($\sigma_{\text{gas}} < \sigma < \sigma_{\text{LE}}$) the film is not uniform; it is a mixture of LE and gas domains. At any point of the film, the surface density is equal either to σ_{LE} or to σ_{gas} ; σ is only an average value. In practice, the range of σ values which can be explored, for an adsorption of polymers to a uniform film, is restricted to $\sigma_{\text{LE}} < \sigma < \sigma_{\text{LC}}$.

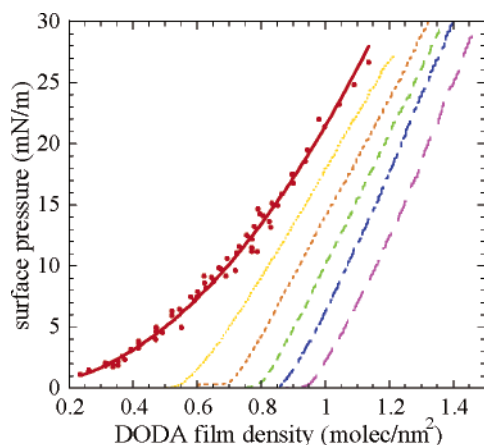


Figure 7. Isotherms of DODA on PAAH solutions, 10^{-4} mol of monomers/L, $T \approx 22^\circ\text{C}$, at different pH values; from right to left: pH = 8.5, pH = 7, pH = 6.5, pH = 5.8, pH = 5.1, pH = 4.8.

Isotherms, Compressibility, and PM-IRRAS as a Function of pH. Figure 7 shows isotherms of DODA films on PAA solutions at room temperature ($\sim 22^\circ\text{C}$) and for different values of pH between 4.8 and 8.5. By increasing the pH, the ionization degree α of the polyacid is varied from ~ 0.1 to ~ 1 . For $\text{pH} > 5$, the isotherms are similar to the one on pure water; in particular, they show a gas–LE plateau. The density at which this coexistence ends, σ_{LE} , increases with the pH. For a given value of the DODA film density, the surface pressure increases when decreasing the pH: the quantity of adsorbed polymers increases when decreasing α . If each counterion of DODA is replaced by a charged monomer of PAA, the total number of adsorbed monomers per unit area, Γ , is expected to be equal to σ/α ; it is indeed expected to increase when α is decreased.

Figure 8a shows the elastic compression moduli ϵ deduced from these isotherms along with that of a DODA film on pure water and on PAAH solutions at pH = 4.8.¹⁵ For clarity, only a few curves are shown. In all these curves, at low DODA film density, the elastic modulus is equal to zero: when compressing the film in the gas–LE plateau, the fraction of LE phase increases at constant pressure. When entering the LE phase, ϵ steeply increases to a finite value. Note that the variations of ϵ are smoothed since they are calculated from a smoothed curve, so that the increase at $\sigma = \sigma_{\text{LE}}$ does not appear abrupt. In the same way, ϵ of DODA on pure water collapses when entering the LE–LC transition, at $\sigma \approx 1.2$ molecules/nm². The case pH ≈ 4.8 differs from the others because the gas–LE transition does not exist or begins for a value of σ below the explored range.

The compression modulus ϵ is higher for DODA films on PAA solutions than on pure water: the mixed DODA–PAA film is more difficult to compress than the DODA film with small counterions. In the same way the film is as stiff as α is low (at least in the beginning of the LE phase). This is again consistent with a quantity of adsorbed polymers as high as α is low. A change in the slope appears in some of the $\epsilon(\sigma)$ curves; it appears more clearly in the $\epsilon(\pi)$ curves (Figure 8b). As discussed for pH = 4.8, this is probably the signature of a change in the conformation of the adsorbed molecules, from flat layer to adsorbed carpet, at $\sigma = \sigma_0(\alpha)$. This was again confirmed by IR spectroscopy. For instance, Figure 9 shows PM-IRRAS spectra at pH =

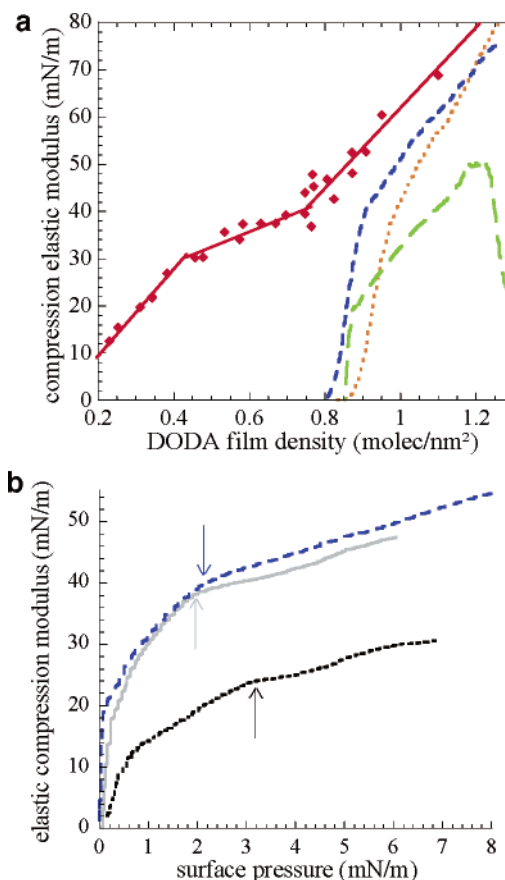


Figure 8. Compression elastic modulus ϵ of DODA films on water and on PAAH solutions, 10^{-4} mol of monomers/L, $T \approx 22^\circ\text{C}$, at different pH values; (a) ϵ as a function of the DODA film density σ , from right to left: water pH = 4 (adjusted with HCl), PAAH solutions pH = 8.2, 7, 4.8; (b) ϵ as a function of the film pressure π , from right to left: PAAH solutions pH = 5.1, 6.5, 7; arrows indicate changes in the slopes of the $\epsilon(\pi)$ curves.

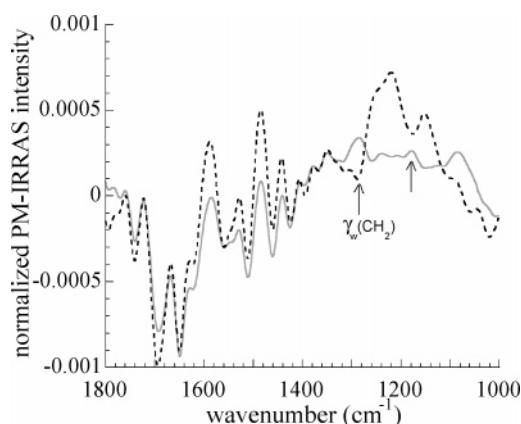


Figure 9. PM-IRRAS spectra of PAAH adsorbed at a DODA Langmuir film from a PAAH solution, 10^{-4} mol of monomers/L, pH = 6.5, $T \approx 20^\circ\text{C}$: plain line, DODA film density $\sigma = 0.75$ molecule/nm²; dashed line, $\sigma = 0.86$ molecule/nm². Two bands (indicated by arrows) have different signs in the two spectra.

6.5 and for two different densities of the DODA film: 0.75 and 0.86 molecule/nm². In the first spectrum the CH₂ wagging band is positively oriented with respect to the baseline (the polymers lie flat at the surface) while it is negatively oriented in the second spectrum (the average orientation of the polymers is orthogonal to the surface).

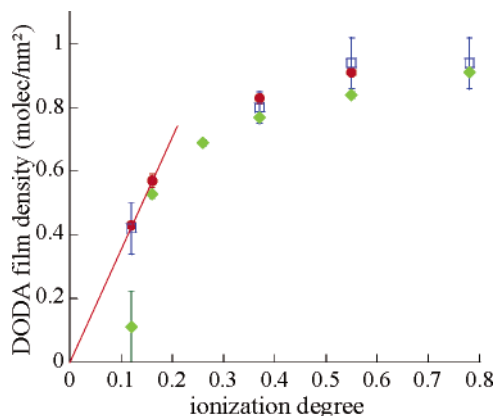


Figure 10. DODA film densities corresponding to the end of the gas–LE transition, σ_{LE} (diamonds), and to the transition in the configuration of the adsorbed polymers, σ_0 , as deduced from the PM-IRRAS spectra (open squares) or by the compression elastic modulus measurements (disks).

Figure 10 summarizes the measured values of σ_{LE} (beginning of the LE phase) and of σ_0 (transition from flat to carpet configuration) as a function of α ; α is the fraction of dissociated COOH groups along a PAA chain in solution, and it was calculated from the concentrations and from the measured pH. The measured values of σ_0 and σ_{LE} are close to each other. This could explain why the signature of σ_0 in the elasticity curves or in PM-IRRAS spectra could not be observed in some of the experiments. The expected value of σ_0 is α/a^2 , where a is the size of the monomer.^{10,11} Such a linear law is compatible with our measurements at low α (see Figure 10). But when increasing α , both σ_{LE} and σ_0 saturate, presumably because α saturates. There are several possible explanations for this phenomenon. The value of α is governed both by the pH and by the local electric field around the polyelectrolyte.²² Both differ at the surface with respect to within the solution, so that the ionization degree of the adsorbed polymers, α_{surf} , probably differs from that of the polymers in solution, α , and could saturate. Unfortunately, as already mentioned, the value of α_{surf} could not be deduced from the PM-IRRAS spectra because of the strong orientation of the COOH groups at the surface. Another possible explanation for the saturation of σ_0 is a saturation of the charge fraction f of the polymer rather than of its ionization degree α , an analogue to the Manning condensation. For polyelectrolytes in solution in water, at low ionization degree, the values of α (fraction of dissociated COOH groups) and f (fraction of monomers carrying a charge) are equal to each other. But when increasing α , some counterions condense on the polymer so that the distance between charged groups always exceeds the Bjerrum length l_B , and f saturates to a/l_B .²³ A similar phenomenon probably occurs at the surface, leading to a saturation of f_{surf} and of σ_0 , which is expected to be equal to f_{surf}/a^2 rather than to α_{surf}/a^2 . Once again, the value of f_{surf} , which is controlled by the local electric field around the adsorbed polyelectrolytes, probably differs

from the value of f for the polyelectrolytes in solution.²⁴ To confirm these hypotheses, independent measurements of the amount of adsorbed sodium ions (for instance by radiolabeling) would be necessary.

Conclusion

We have evidenced by elasticity measurements and by PM-IRRAS that the conformation of polyelectrolytes adsorbed at oppositely charged surfaces depends both on the surface and on the polyelectrolyte charge densities. This result could be used for a better control of the properties of adsorbed polymers. Nevertheless, the system we used is very particular (air–water interface, weak polyelectrolyte in theta-solvent condition, relatively short chains, low salinity). The results need to be generalized, for instance, by a systematic study of the effect of temperature, chain length, and salinity.

Acknowledgment. The authors are indebted to J. Meunier for the use of Brewster angle microscopy.

References and Notes

- (1) Fleer, G. J.; Cohen Stuart, M. A.; Scheutjens, J. M. H. M.; Cosgrove, T.; Vincent, B. *Polymers at Interfaces*; Chapman and Hall: London, 1993.
- (2) Eisenriegler, E. *Polymers Near Surfaces*; World Scientific: Singapore, 1993.
- (3) Decher, G. *Science* **1997**, *277*, 1232.
- (4) For a review see: Netz, R.; Andelman, D. *Phys. Rep.* **2003**, *380*, 1.
- (5) Ahrens, H.; Baltes, H.; Schmitt, J.; Möhwald, H.; Helm, C. A. *Macromolecules* **2001**, *34*, 4504.
- (6) Tronin, A.; Lvov, Y.; Nicolini, C. *Colloid Polym. Sci.* **1994**, *272*, 1317.
- (7) McAloney, R. A.; Goh, M. C. *J. Phys. Chem. B* **1999**, *103*, 10729.
- (8) Sukhishvili, S. A.; Dhinojwala, A.; Granick, S. *Langmuir* **1999**, *15*, 8474.
- (9) Park, S.; Barrett, C.; Rubner, M.; Mayes, A. *Macromolecules* **2001**, *34*, 3384.
- (10) Dobrynin, A. V.; Deshkovski, A.; Rubinstein, M. *Phys. Rev. Lett.* **2000**, *84*, 3101.
- (11) Dobrynin, A. V.; Deshkovski, A.; Rubinstein, M. *Macromolecules* **2001**, *34*, 3421.
- (12) Brandrup, J.; Immergut, E. H.; Grulke, E. A.; Abe, A.; Bloch, D. R. In *Polymer Handbook*, 4th ed.; John Wiley and Sons: New York, 1999.
- (13) Lheveder, C.; Hénon, S.; Mercier, R.; Tissot, G.; Fournet, P.; Meunier, J. *Rev. Sci. Instrum.* **1998**, *69*, 1446.
- (14) Blaudez, D.; Buffeteau, T.; Cornut, J.-C.; Desbat, B.; Escafre, N.; Pezolet, M.; Turlet, J.-M. *Appl. Spectrosc.* **1993**, *47*, 869.
- (15) Vagharchakian, L.; Hénon, S. *Langmuir* **2003**, *19*, 7989.
- (16) Leyte, J. C.; Zuiderweg, L. H.; Vledder, H. J. *Spectrochim. Acta, Part A* **1967**, *23*, 1397.
- (17) Le Calvez, E.; Blaudez, D.; Buffeteau, T.; Desbat, B. *Langmuir* **2001**, *17*, 670.
- (18) Novak, A. In *Structure and Bonding*; Springer-Verlag: Berlin, 1974; Vol. 18.
- (19) Xie, A. F.; Granik, S. *Nat. Mater.* **2002**, *1*, 129.
- (20) Ahuja, R. C.; Caruso, P. L.; Möbius, D. *Thin Solid Films* **1994**, *242*, 195.
- (21) Taylor, D. M.; Dong, Y.; Jones, C. C. *Thin Solid Films* **1996**, *284/285*, 130.
- (22) Mandel, M. In *Chemistry and Technology of Water Soluble Polymers*; Finch, C. A., Ed.; Plenum Press: New York, 1983.
- (23) Manning, G. S. *J. Chem. Phys.* **1969**, *51*, 924.
- (24) Sens, P.; Joanny, J.-F. *Phys. Rev. Lett.* **2000**, *84*, 4862.

MA048540U